ARTICLE

Crystal Structure and Photocatalytic Characteristics of Nanoscale Sb-doped TiO_2 Thin Films

Da-sen Ren[a,b*], Zhuang-jian Zhang[a]

a. Department of Materials Science, Fudan University, Shanghai 200433, China; b. Computer Center, Guizhou University for Ethnic Minorities, Guiyang 550025, China

(Dated: Received on March 29, 2006; Accepted on September 25, 2006)

Nanoscale Sb doped titanium dioxide thin films photocatalyst ($Ti_{1-x}SbO_2$) were obtained from dip-coating sol-gel method. The influence of dopant Sb density on the crystal structure and the phase transformation of the thin films were characterized by X-ray diffraction (XRD) and Raman spectra. The results of XRD showed that as-prepared films were not only in anatase state but also in brookite. The crystalline size was estimated to be around 13.3-20 nm. Raman spectra indicated there coexisted other phases and a transformation from brookite to anatase in the samples doped with 0.2% Sb. After doping a proper amount of Sb, the crystallization rate and the content of the anatase $Ti_{1-x}SbO_2$ in the thin films was clearly enhanced because Sb replaced part of the Ti of TiO_2 in the thin films. The anode current density (photocurrent density) and the first order reaction speed constant (k) of thin films doped with 0.2% Sb reached 42.49 $\mu A/cm^2$ and 0.171 h/cm^2 under 254 nm UV illumination, respectively, which is about 11 times and 2 times that of the non-doped TiO_2 anode prepared by the same method respectively.

Key words: Crystal structure, XRD pattern, Raman spectra, Anatase, Dopant, Anode current density

I. INTRODUCTION

Titanium dioxide photo catalysis has been studied profusely in recent years due to its high photocatalytic rate, and its chemical and photoelectrochemical durability. However, TiO_2 can only absorb approximately 5% of the solar light reaching its surface because of its large band gap of about 3.2 eV. Therefore, a high utilization of solar energy has become a critical problem not only in the field of TiO_2 solar cells, but in the superhydrophilicity and photocatalytic activity of TiO_2 thin films as well. To encourage the production of photo-generated electron-hole pairs, and simultaneously inhibit their recombination, much effort has been made by producing transition bands to promote the dissociation of electron-hole pairs and help the electrons transfer to the conduction band. For example, surface modification by dye adsorption [1,2] and metal dopant introduction [3-9] have been widely tried to extend the photo-response to the visible region of solar spectrum. Nevertheless, the conversion efficiency is hard to enhance because of the following reasons [10]: Firstly, Schottky barriers form between the host electrodes and the dopants, so that the electron transfer is retarded. Secondly, the dopants serve as recombination centers for the photo-induced electron-hole pairs. In 2001, however, Asahi *et al.* [11] introduced N to TiO_2 thin films. The as-doped $TiO_{2-x}N_x$ composite semiconductor had a conspicuous photo-response to visible light with wavelengths near 500 nm. It was a breakthrough in utilizing the solar energy. After it, Khan *et al.* [12] synthesized a chemically modified n-type TiO_2 by controlled combustion of Ti metal in a natural gas flame. The CM-n-TiO_2 photocatalyst absorbs light at wavelengths below 535 nm and has a 2.32 eV band-gap energy. In this work, Sb is used as the dopant of TiO_2 thin films, for the ionic radius of 6-fold coordinated Sb^{5+} with 74 μm [13] is very close to that of octahedrally coordinated Ti^{4+} in anatase and rutile TiO_2 crystal [14] with 74.5 μm [13]. It is very possible for Sb^{5+} to occupy the substitution site in a TiO_2 anatase or rutile matrix to form $Ti_{1-x}Sb_xO_2$ composite.

Our previous work [15,16] placed a major emphasis on the superhydrophilicity of $Ti_{1-x}SbO_2$ thin films prepared on glass by a sol-gel procedure. It indicated that after doping with a proper amount ($\leq$0.2%) of Sb, TiO_2 thin films turned out to have more outstanding superhydrophilicity than pure ones. The water contact angle of the sample with 0.2% Sb promptly decreased to zero degrees after 254 nm UV irradiation for 1 h with a power density of about 90-95 $\mu W/cm^2$. In this study, photocatalytic properties of the ITO/$Ti_{1-x}SbO_2$ electrodes will be analyzed by cyclic voltammetric behavior and the photo-induced dissociation of methylene blue. A phase transformation illustrated by XRD patterns and Raman spectra is put forward to clarify the effect of Sb on the crystal structure and the photoelectrochemical properties of TiO_2 thin films.

*Author to whom correspondence should be addressed. E-mail: dsren@mail.gznc.edu.cn, senrd@vip.sina.com

II. EXPERIMENTS

A. Preparation of $Ti_{1-x}SbO_2$ samples

The reagents tetra-*n*-butyl titanate ($(C_4H_9O)_4Ti$, $\geq$98.0%), acetylacetone ($C_5H_8O_2$, $\geq$98.5%), ethyl alcohol (C_2H_5OH, $\geq$99.7%), $SbCl_3$ ($\geq$99%) and deionized water are used in the sol-gel method. The preparation procedures of Sb doped titanium dioxide sol were as follows.

(i) Dissolve 4 mL tetra-*n*-butyl titanate in $(22.2-x)$ mL of ethyl alcohol. Solution A is formed after stirring it in air for 10 min.

(ii) Certain amounts of $SbCl_3$ crystals are introduced into x mL of ethyl alcohol. Solution B is obtained after they are completely dissolved by stirring in air.

(iii) Acetylacetone (4 mL) used as peptizant is slowly added into the mixed solution of A and B (1:1), and followed by the introduction of 1 mL deionized water for hydrolysis.

(iv) After stirring in air for 1 h, the TiO_2:Sb sol is finally formed. It has a yellow color.

Uniform coatings of TiO_2: Sb on clean glass and ITO have been obtained by dipping in the solution, and withdrawing at a speed around 2.6 mm/s. After drying at room temperature for 48 h, glass/$Ti_{1-x}SbO_2$ samples and ITO/$Ti_{1-x}SbO_2$ electrodes are all subjected to thermal treatment up to 450 °C in air for 1 h.

Samples derived from the solutions with different $SbCl_3$ concentrations of 0.0, 0.05%, 0.1%, 0.2% and 1.0% are denoted as A, B, C, D and E, respectively.

B. Characterization

The crystalline structure of the thin films was investigated by X-ray diffraction (XRD) and Raman scattering experiments. A Rigaku D/MAX-rB X-ray diffractometer with Cu Kα radiation operated at 40 kV and 100 mA was employed to observe the XRD patterns. Raman spectra was obtained from a Dilor LabRam-1B Raman microprobe using the He–Ne 632.8 nm line.

C. Photoelectrochemical measurements

Photoelectrochemical measurements were carried out in an electrolytic cell with a quartz window. It was composed of the ITO/TiO_2: Sb electrode, a saturated calomel electrode (SCE) and a Pt flat electrode as the working, reference and counter electrodes, respectively. The area of the working electrodes was 0.5 cm^2. A solution of 0.5 mol/L Na_2SO_4 was used as the supporting electrolyte. The cyclic voltammograms were successively scanned at the scanning rate of 0.05 V/s by a CHI660 electrochemical workstation (CH Instrument Inc., 3700 Tennison Hill Drivel Austin, USA). Two 8 W UV lamps with wavelengths around 254 and 365 nm, and a 120 W Xe lamp were used for illuminating the electrode samples.

III. RESULTS AND DISCUSSION

A. XRD patterns and Raman spectra

The XRD patterns of samples with different Sb concentrations are presented in Fig.1. A distinctive anatase (101) peak at 2θ=25.3° in all samples indicated that the $Ti_{1-x}SbO_2$ thin films had a majority of anatase structure. However, some other phases coexisted apart from anatase, such as brookite, as implied by the brookite (121) peak (2θ=30.9°). The crystalline size of these samples was estimated to be 13.3-20 nm by use of the Scherrer equation.

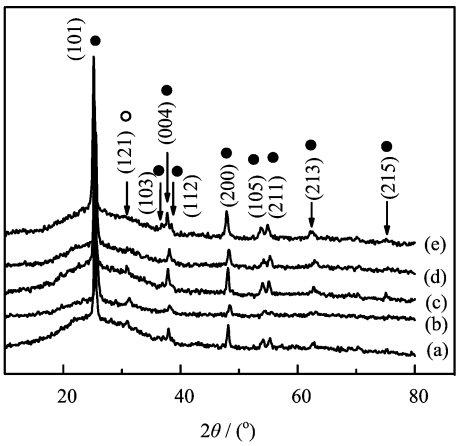

FIG. 1 XRD patterns of TiO_2 thin films with different Sb concentrations. (a) 0.0%, (b) 0.05%, (c) 0.1%, (d) 0.2%, (e) 1.0% ("•" anatase, "○" brookite).

Anatase TiO_2 belongs to space group $D_{4h}^{19}(I4_1/amd)$, and each cell includes two TiO_2 molecules. Table I shows the Raman vibrating frequency of anatase TiO_2 [17].

TABLE I The frequency of active vibrating model for the general multicrystal and singlecrystal anatase TiO_2

Multi-crystal/cm^{-1}	Single-crystal/cm^{-1}	Vibration model
143	144	E_g
196	197	E_g
392	400	B_{1g}
510	515	B_{2g}
633	640	E_g

The Raman spectra in Fig.2 provide more detailed information. The Raman lines at 146, 199, 398, 517 and 638 cm^{-1} can be assigned to anatase phase as E_g, E_g, B_{1g}, B_{2g} and E_g modes [18,19], respectively. The peaks at 215, 246, 323 and 366 cm^{-1} are attributed to brookite

ISSN 1003-7713/DOI:10.1360/cjcp2006.19(6).549.6

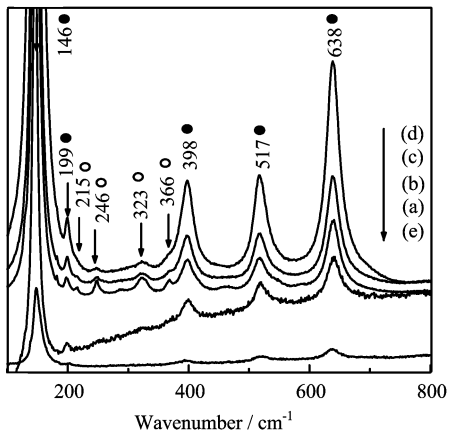

FIG. 2 Raman spectra of the samples with different Sb concentration. (a) 0.0%, (b) 0.05%, (c) 0.1%, (d) 0.2%, (e) 1.0% ("•" anatase, "○" brookite).

phase [18,20]. The strongest E_g mode at 146 cm^{-1} indicates that an anatase phase was formed in all samples. This conclusion is in good agreement with the XRD results shown in Fig.1. When Sb concentration is increased to 0.2%, the intensity of brookite peaks decreases drastically accompanied by an up-forward tendency of the anatase peaks. However, when Sb is further increased to 1%, the Raman peaks intensity of anatase TiO_2 finally diminishes and the brookite peaks disappear.

It can be seen from Fig.2 and Table I that the Raman lines of E_g at 146 and 199 cm^{-1} nanoscale anatase TiO_2 have a 2 cm^{-1} blueshift compared to the frequency of the single bulk crystal anatase TiO_2 (shown in Table I). The blueshift phenomenon has two possible explanations. One is that the grain size of the nanoscale materials is smaller than the bulk materials, and another is that it is induced by the oxygen vacancy, which was produced in the process of preparing TiO_2. Parker *et al.* annealed TiO_2 at different temperatures in an Ar atmosphere so that different grain size of TiO_2 was observed [21]. The result showed that Raman frequencies had not changed. However, after TiO_2 was annealed in a vacuum, the Raman lines were changed distinctly. So they thought that the blueshift of the Raman line was induced by the oxygen vacancy in the TiO_2. But Zhang *et al.* [18] and Bersani *et al.* [23] calculated the lowest-frequency Raman spectra of the E_g mode in anatase TiO_2 under the phonon confinement model at different grain sizes, respectively. The results showed that as the crystalline size decreased, the frequency and linewidth of the E_g Raman peak blueshifted and increased, respectively. The calculated results based on the phonon confinement model were in qualitative agreement with their experimental data. This indicates that the phonon confinement is the dominant mechanism responsible for the blueshift and broadening of the Raman peak in small-sized nanocrystals. In our experiment, all samples were annealed in an oxygen atmosphere, so the the possibility of oxygen vacancy in the samples is very small. Therefore, we think that the blueshift of the Raman peaks shown in Fig.2 is caused by the small nanocrystal size.

Figure 3 shows the results of the scattered intensity of Raman peaks at 146 cm^{-1} against the Sb concentration. The scattered intensity of Raman peaks in anatase increases with the increase of Sb. When Sb concentration reaches 0.2%, the scattered intensity of Raman peaks at 146 cm^{-1} in anatase TiO_2 becomes maximal. However, the scattered intensity of Raman peaks decreases drastically accompanied by an up-forward tendency in the intensity of anatase peaks. The Raman peaks intensity of anatase TiO_2 finally diminishes and the brookite peaks disappear, when the concentration of Sb is further increased to 1%. This indicates that the optimal concentration of Sb is 0.2%. These results are in qualitative agreement with the results of XRD.

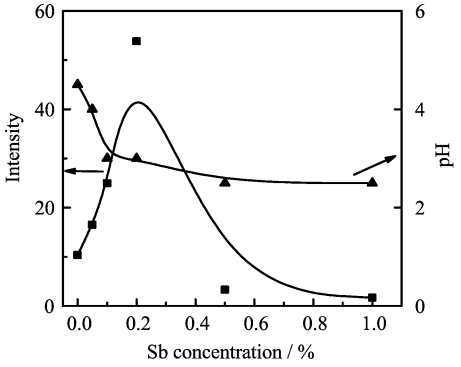

FIG. 3 Scattered intensity of Raman peak at 146 cm^{-1} and the pH value of sol on the different Sb concentration doped-in TiO_2 thin films.

Hu *et al.* measured the Raman spectra of TiO_2 powder prepared by hydrolyzing $TiCl_4$ [19]. The results indicated that the brookite phase existed in Raman spectra of the TiO_2 powders after heat treatment at 450 °C for 2 h at the pH values from 2 to 5. The intensity of the shift bands of brookite phase became weaker with increasing the synthesized pH value. The brookite phase disappeared completely when pH value increased to 8. It was found that the *c* parameter and *a* parameter decreased with increasing the pH value. They thought that the lattice change of anatase phase could be induced by microstrains for oxygen vacancy, hydrostatic pressure or specific cations. The results of the weight change of the TiO_2 powders under heating showed that the most probable explanation for the changes in lattices of anatase was the strain under hydrostatic pressure. In the procedure for preparation of the TiO_2:Sb sol, the pH value of the sol varied with the Sb increase as shown in Fig.3.

The pH value of pure TiO_2 sol is about 4.5. The pH value of the TiO_2:Sb sol decreases with the increase of Sb. The pH value decreases to 2.5 after the dopant Sb

ISSN 1003-7713/DOI:10.1360/cjcp2006.19(6).549.6

reaches 1%. The pH value varying with Sb density may have two possible explanations. One is that the dopant $SbCl_3$ reacted with the water in sol (shown in formation (1)).

$$SbCl_3+3H_2O \rightarrow Sb(OH)_3+3HCl \quad (1)$$

The reaction product HCl may change the pH value of the sol. The other explanation is that the complex oxide showed higher acidity than the single oxide because a new acidity acurred after two kinds of oxide forming one phase for the diversity in coordinate and electronegative of different metals . When the substitution led to surplus negative electronic charge, the semiconductor attracted protons and formed Bronst acidity. But if the substitution led to surplus positive electronic charge, Lewis acidity formed [24]. However, it can be found from Fig.2 and Fig.3 that the brookite peaks decline with the up-forward shift of Sb from 0 to 0.2%. Therefore, the actual reason for the intensity change of anatase peaks is not induced by the pH value of the sol, but relates directly to the dopant Sb. In other words, although the change of brookite peaks with Sb density is similar to the change of brookite peaks with the pH value reported in the literature [14], they have different causes. Because Sb^{5+} with the radius of 74 μm is very close to the radius of Ti^{4+} (74.5 μm) [25], therfore Sb substitutes for part of the Ti in TiO_2 to form $Ti_{1-x}Sb_xO_2$ structure. As analyzed above, we think that the change of the brookite peaks shown in Fig.2 may be caused by Sb coming into TiO_2 to bring about the change of the parameters of lattice.

Additional information about Sb can be obtained from Fig.4. In the enlarged part of the Raman spectra, an Sb–O line at 181 cm^{-1} exists in samples B-D [26] and an Sb–Sb line at 138 cm^{-1} appears in sample E [27]. The former Raman line at 181 cm^{-1} resulted from a combination of Sb and O in TiO_2 to form an Sb-O bond, and the latter one at 138 cm^{-1} is ascribed to an Sb-Sb bond formed from interaction between two Sb atoms. The structure of Sb–Sb destroyed the crystal structure of the TiO_2 anatase [28].

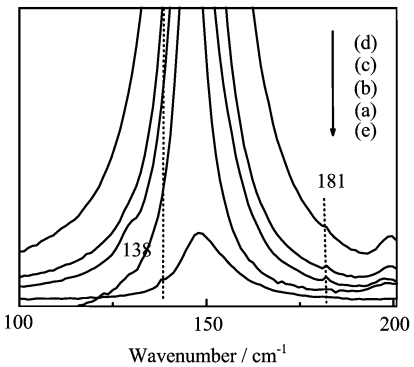

FIG. 4 The enlarged part of Raman spectra. (a) 0.0, (b) 0.05%, (c) 0.1%, (d) 0.2%, (e) 1.0%.

B. *In-situ* photoelectric response

Figure 5 shows the cyclic voltammetric curves of the ITO/$Ti_{1-x}Sb_xO_2$ electrodes with different Sb concentrations (0, 0.2%, 1%) before (UV off) and under 254 nm UV (Fig.5(A)), 365 nm UV (Fig.5(B)) and GX-5 120 W Xe (Fig.5(C)) irradiation. The distance between the source of light and the quartz window was about 6 cm. It has been demonstrated that the anodic current density I represents the anodic photocurrent density [16,23]. Under 254 nm UV illumination, the anodic photocurrent density of the electrodes with 0.2% and 1% Sb approaches 42.49 and 35.73 $\mu A/cm^2$, increases of 10.9 and 9.2 times respectively compared to a pure TiO_2/ITO electrode with a current density of 3.89 $\mu A/cm^2$ (Fig.5(a)). This suggests that Sb doped electrodes have a higher photoelectric conversion rate than non-doped ones, especially for the ones with Sb concentration of 0.2%.

As seen in Fig.5(B) and Fig.5(C), similar results were obtained when the illumination source changed to a 365 nm UV Fig.5(B) and a GX-5 120 W Xe lamp Fig.5(C). The photocurrent density of 0.2% Sb doped electrode reaches 9.03 and 99.34 $\mu A/cm^2$ respectively, which represents a much higher photoelectric conversion rate when it was exposed to the full range of the solar spectrum. It also can be found from Fig.5 that the TiO_2 thin film electrode doped with the same Sb concentration has different photoelectric conversion rates under different illumination sources. For example, the electrode with 0.2% Sb has its highest photoelectric conversion rate under GX-5 120W Xe lamp irradiation with anode photocurrent density of 99.34 $\mu A/cm^2$. The photoelectric conversion rate under 254 nm UV irradiation takes second place with the photocurrent density of 42.49 $\mu A/cm^2$, and it is the lowest under 365 nm UV irradiation. The difference of the photoelectric conversion rate under diverse illumination source may have two reasons [29]. One is the different absorbance of the TiO_2 thin film to diverse UV light. The transmission rate of the TiO_2 thin film on quartz glass to 254 and 365 nm UV light was tested by a UV light power densimeter made by Beijing Normal University of China. The results show that the transmission rate of TiO_2 thin film to 365 nm UV light reaches 81%, greater than to 254 nm UV light with the transmission rate of 18%, which means that the TiO_2 thin film has much higher absorbance to 254 nm UV light than to 365 nm UV light. The second reason could be that the photon of the 254 nm light has higher energy, which excites the electron from the valence band of the TiO_2 to the conduction band so that the electron-hole pair has much high kinetic energy, which may have a positive effect on the photoelectron conversion rate.

The samples have higher anode photocurrent under Xe light irradiation than under 254 and 365 nm UV light irradiation, which has two reasons. The first reason is the wide wave range, from ultraviolet light to visible

ISSN 1003-7713/DOI:10.1360/cjcp2006.19(6).549.6

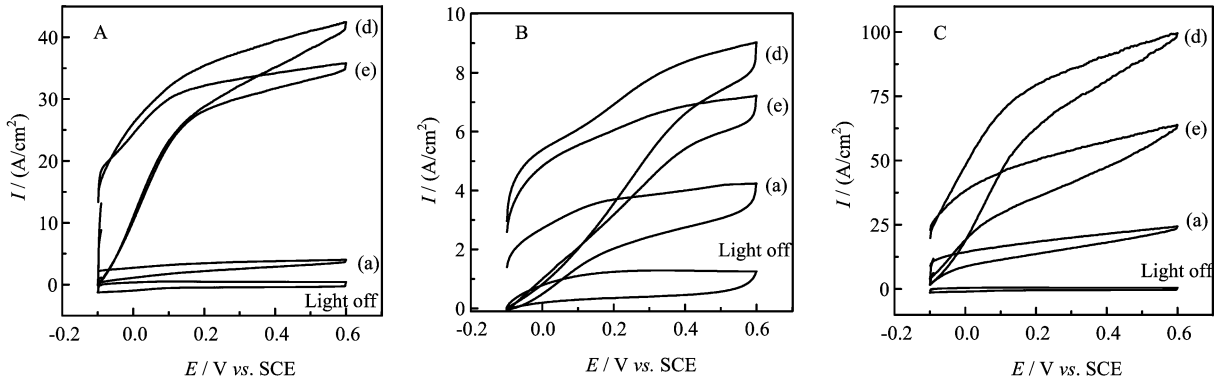

FIG. 5 Cyclic voltammograms at 0.05 V/s for the electrodes (a) 0.0%, (d) 0.2%, (e) 1.0% with different Sb concentrations with and without light. A. 254 nm UV light, B. 365 nm UV light, C. GX-5 120 W Xe lamp.

light, of XE emitted, so that the wave light range of TiO_2 thin film response is increased. Another reason is that the photon power density of Xe emitted is greater than the separate UV light emitted, and the photocurrent density is in direct ratio to the photo power density. For example, the anode photocurrent density of the TiO_2 thin film electrode with 0.2% Sb under 245 nm UV irradiation reached 102.50 μA/cm^2 when the distance from light to quartz window was decreased to 1 cm to increase the photo power density.

C. The photocatalytic activity of $Ti_{1-x}Sb_xO_2$ thin film

The photocatalytic activity of the $Ti_{1-x}Sb_xO_2$ thin films with different Sb concentration of 0, 0.2% and 1.0% were characterized by the decomposition of methylene blue. The $Ti_{1-x}Sb_xO_2$ thin films were immersed in 12 μmol/L methylene blue solution and illuminated by a 254 nm UV lamp with a power density of 280-290 μm/cm^2. The absorbency of the solution was measured by a SM240 spectrophotometer (made by CVI). The results depending on the UV irradiation time are shown in Fig.6. The experimental results show that the all samples have strong photocatalytic capability for the methylene blue. After irradiation for 120 min, about 90% of the methylene blue was decomposed by the thin films with 0 and 1.0% Sb while the methylene blue in the solution was almost decomposed by the $Ti_{1-x}Sb_xO_2$ thin film with 0.2% Sb. Therefore the thin film with 0.2% Sb shows stronger photocatalytic activity for methylene blue than other thin films.

It can be seen from Fig.6 that $\ln(A/A_0)$ (A_0 is the initial absorbency and A is the absorbency of the solution after irradiation for some time) is almost in linear in relation ship with the reaction time. So the decomposition effect of the $Ti_{1-x}Sb_xO_2$ thin films on methylene blue is almost the first order. Although all samples with different Sb concentration have strong decomposition capability for methylene blue, the difference in their decomposition speeds is observable (shown in Fig.6). The slope (reaction speed constant) of the thin film doped with 0.2% Sb is bigger than the slopes of samples with 0 and 1% Sb. The reaction speed constant k of the three kinds of samples (with 0, 0.2% and 1% Sb) is 0.095, 0.171 and 0.110 h/cm^2 respectively. This means that the sample with 0.2% Sb has stronger photo-induced catalysis than other two samples (with 0 and 1%). At the same time, this result is in accord with the anode photocurrent density with different Sb concentration under UV illumination (shown in Fig.5).

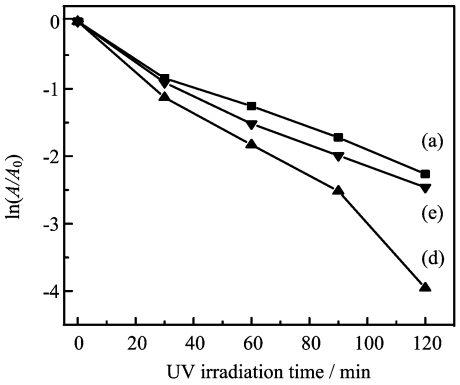

FIG. 6 The decomposition of methylene blue by $Ti_{1-x}Sb_xO_2$ thin films with different Sb concentration, by UV irradiation time. (a) 0.0%, (d) 0.2%, (e) 1.0%

It is known that only the anatase and rutile TiO_2 have photocatalicity in the three kinds crystalline structure of titanium dioxide. It can be seen from Fig.1 and Fig.2 that rutile structure does not appear in the $Ti_{1-x}Sb_xO_2$ thin films with different Sb concentration prepared in these conditions, so the photocatalysis of methylene blue by the thin films is mainly induced by the content of anatase, the crystal size and the light absorbance range. However, there is hardly any change in the crystal size (in Fig.1) and in the absorbance spectrum (the figure is omitted), so the different photocatalytic activity of $Ti_{1-x}Sb_xO_2$ thin films with diverse Sb concentration on methylene blue is mostly caused

ISSN 1003-7713/DOI:10.1360/cjcp2006.19(6).549.6

by the relative content of the anatase. Because the anatase TiO_2 in the thin film with 0.2% Sb has the highest crystal efficiency in thin films, therfore it also has best photo-induced catalysis.

IV. CONCLUSION

$Ti_{1-x}Sb_xO_2$ thin films and electrodes were prepared by the dip-coating sol-gel method. The following conclusions are obtained.

(i) After doping with a proper amount of Sb, the Sb-O-Ti structure is formed with Sb substituting for some Ti in TiO_2 so that the crystal lattice parameter (a,c) may be changed, the crystal efficiency of the thin film is enhanced, and the relative content of anatase $Ti_{1-x}Sb_xO_2$ is increased. However, in the $Ti_{1-x}Sb_xO_2$ thin films with Sb concentration over 0.2%, the dominant structure of Sb–Sb bonds destroys the anatase structure. Therefore, the optimal concentration is found to be 0.2% with the maximum crystal efficiency.

(ii) The photoelectric conversion efficiency has been improved after doping with Sb. The photocurrent density of the electrode with 0.2% Sb is about 42.49 $\mu A/cm^2$ under 254 nm UV irradiation with the power density of about 375 $\mu W/cm^2$, which is about 11 times greater than the non-doped TiO_2 thin film electrode prepared in the same conditions.

(iii) The experimental results of the decomposition of methylene blue show that although the absorbance spectrum is not be shifted to visible range, the photocatalytic activity of the thin films has been substantially improved after doping with 0.2% Sb. The reaction speed constant k of the thin film with 0.2% to 10 μmol/L methylene blue solution is 0.171 h/cm^2 under 254 nm UV irradiation with the power density of 230 $\mu W/cm^2$, which is 2 times the reaction speed constant k of the non-doped TiO_2 thin film prepared in the same conditions.

V. ACKNOWLEDGMENTS

This work was supported by the Department of Education of Guizhou Province and the Ministry of Education of China (206134).

[1] N. Negishi, K. Takeuchi and T. Ibusuki, Appl. Surf. Sci. **121/122**, 417 (1997).
[2] Z. S. Sun, Y. X. Chen, Q. Ke, Y. Yang and J. Yuan, J. Photochem. Photobio. A: Chem. **149**, 169 (2002).
[3] L. Jun, C. Y. Jimmy, D. Lo and S. K. Lam, J. Catal. **183**, 368 (1999).
[4] X. Z. Li, F. B. Li, C. L. Yang and W. K. Ge, J. Photochem. Photobio. A: Chem. **141**, 209 (2001).
[5] Enrico Traversa, Maria Luisa di Vona, Patrizia Nunziante, Silvia Licoccia, Jong-Won Yoon, Takeshi Sasaki and Naoto Koshizaki, J. Sol-Gel Sci. & Tech. **22**, 115 (2001).
[6] X. Z. Li and F. B. Li, J. Appl. Electrochem. **32**, 203 (2002).
[7] M. Z. Atashbar, H. T. Sun, B. Gong, W. Wlodarski and R. Lamb, Thin Solid Films **326**, 238 (1998).
[8] C. Zhao and S. H. Zhong, Chin. J. Chem. Phys. **18**, 273 (2005).
[9] C. S. Mei and S. H. Zhong, Chin. J. Chem. Phys. **18**, 822 (2005).
[10] Y. V. Pleskov and A. M. Kraitsberg, Sol. Energy Mater. **22**, 119 (1991).
[11] R. Asahi, T. Morikawa, T. Ohwaki, K. Aoki and Y. Taga, Science **293**, 269 (2001).
[12] S. U. M. Khan, Al-Shahry Mofareh and B. Jr. William, Science **297**, 2243 (2002).
[13] R. D. Shannon, Acta Crystallogr. **A32**, 751 (1976).
[14] C. J. Howard, T. M. Sabine and F. Dickson, Acta Crystallogr B **47**, 462 (1991).
[15] D. S. Ren, Z. M. Bei, L. Huang, J. Shen, X. L. Cui, X. L. Yang and Z. J. Zhang, Acta Phys. Chim. Sinica. **17**, 414 (2004).
[16] Z. M. Bei, D. S. Ren, X. L. Cui, J. Shen, X. L. Yang and Z. J. Zhang, J. Mate. Res. **19**, 3189 (2004).
[17] R. Copwell, J. Appl. Spectroscopy **26**, 537 (1972).
[18] W. F. Zhang, Y. L. He, M. S. Zhang, Z. Yin and Q. Chen, J. Phys. D: Appl. Phys. **33**, 912 (2000).
[19] Y. Hu, H. L. Tsai and C. L. Huang, J. Eur. Ceram. Soc. **23**, 691 (2003).
[20] G. A. Tompsett, G. A. Bowmaker and R. P. Cooney, J. Raman Spectro. **26**, 57 (1995).
[21] J. C. Parker and R. W. Siegel, Appl. Phys. Lett. **57**, 943 (1990).
[22] W. F. Zhang, Y. L. He, M. S. Zhang, Z. Yin and Q. Chen, J. Phys. D: Appl. Phys. **33**, 912 (2000).
[23] D. Bersani, P. P. Lottici and X. Z. Ding, Appl. Phys. Lett. **72**, 73 (1998).
[24] K. Tanabe, Bull. Chem. Soc. Jpn. **47**, 1064 (1974).
[25] R. D. Shannon, Acta Crystallogr **A32**, 751 (1976).
[26] R. Anushree, M. Komatsu, K. Matsuishi and S. Onari, J. Phys. Chem. Solids **58**, 741 (1997).
[27] M. O. Guerreto-Perez, J. L. G. Fierro, M. A. Vicente and M. A. Banares, J. Catal. **206**, 339 (2002).
[28] K. Hinrichs, J. R. Power, N. Esser and W. Richter, Appl. Surf. Sci. **166**, 185 (2000).
[29] X. L. Cui, S. T. Wo, D. S. Ren, J. Shen, X. L. Yang and Z. J. Zhang, Acta Chim. Sini. **61**, 1872 (2003).

ISSN 1003-7713/DOI:10.1360/cjcp2006.19(6).549.6